AIP | The Journal of Chemical Physics

Photodissociation dynamics of water containing clusters. I. KrH2O+

HS. Kim, CH. Kuo, and M. T. Bowers

Citation: The Journal of Chemical Physics **93**, 5594 (1990); doi: 10.1063/1.459630
View online: http://dx.doi.org/10.1063/1.459630
View Table of Contents: http://scitation.aip.org/content/aip/journal/jcp/93/8?ver=pdfcov
Published by the AIP Publishing

Photodissociation dynamics of water containing clusters. I. $Kr \cdot H_2O^+$

H-S. Kim, C-H. Kuo, and M. T. Bowers
Department of Chemistry, University of California, Santa Barbara, California 93106

(Received 12 March 1990; accepted 26 June 1990)

The mass selected $Kr \cdot H_2O^+$ cluster is photodissociated in the range 514 to 357 nm using lines from an argon ion laser. Product branching ratios are measured and shown to be a strong function of photon wavelength; Kr^+/H_2O products dominate at 357 nm (90%) but are equal in intensity to H_2O^+/Kr products at 514 nm. A small KrH^+/OH product is observed at all wavelengths ($\sim$5%), representing the first observation of a photoinduced, intracluster proton transfer reaction. The total cross section is estimated to be $\sim 2\times 10^{-19}$ cm^2 at 514 nm. Laser polarization studies indicated the Kr^+/H_2O products come from direct accessing of a repulsive upper state (intracluster charge–transfer reaction). Both $Kr^+(^2P_{3/2})$ and $Kr^+(^2P_{1/2})$ spin–orbit states are formed, but their branching ratio is very strongly dependent on wavelength: 100% $Kr^+(^2P_{3/2})$ at 514 nm, 100% $Kr^+(^2P_{1/2})$ at 357 nm, and variable amounts of each in between. Analysis of the kinetic energy distribution of Kr^+/H_2O products indicates H_2O is strongly rotationally excited (0.18 to 0.23 eV). This fact, coupled with analysis from an impulsive model for Kr^+–H_2O dissociation suggests the Kr atom is above (or below) the H_2O^+ plane in the $Kr \cdot H_2O^+$ ground state, situated closer to the O end of the molecule. Further analysis of the Kr^+/H_2O kinetic energy distribution yields the binding energy $D_0^0(Kr\text{–}H_2O^+) = 0.33 \pm 0.1$ eV. Polarization studies indicate H_2O^+/Kr products arise from a bound upper state. Phase space theory modeling of the kinetic energy distribution indicates the H_2O^+ product is formed with $\sim$1.3 eV internal energy. Two models are discussed, one that suggests $H_2O^+(\tilde{A}\ ^2A_1)$ is formed and a second that suggests H_2O^+ is the chromophore, internally converts to vibrationally hot $H_2O^+(\tilde{X}\ ^2B_1)$ and slowly leaks vibrational energy to the cluster as a whole before dissociating. The KrH^+/OH products are formed via statistical vibrational predissociation of a bound state and a possible mechanism is discussed.

I. INTRODUCTION

Small gas phase ionic clusters are interesting species from a number of points of view. From a practical standpoint they are important species in the chemistry of earth's atmosphere[1] and in nucleation of gases to liquids.[2] From a fundamental point of view they are interesting because the cluster bond strengths fall in the range 0.1 to 1.3 eV,[3] much stronger than van der Waals bonds (typically 0.01 to 0.1 eV) and weaker than α and π bonds (2 to 5 eV).

In the past five years we have investigated the photodissociation dynamics of 20 to 25 small cluster ions.[4] The studies have been primarily concerned with locating the electronic excited states of the clusters, determining their character (bound, repulsive), determining product energy disposal and product branching ratios, and in favorable cases, determining photodissociation cross sections, qualitative cluster structure, and details of the cluster dissociation mechanism.

In these many studies threads of similarity exist. One such thread is the fact dissociation always occurred with the cluster moieties intact

$$AB^+ + h\nu \rightarrow A^+ + B \quad (1a)$$

$$AB^+ + h\nu \rightarrow B^+ + A, \quad (1b)$$

i.e., no intracluster structural rearrangement occurred before dissociation to products. This was not too surprising because many systems dissociated primarily via repulsive states and that in almost all cases the photon was absorbed into a cluster state not into one of the states associated with the isolated cluster moieties A or B.[5,6]

A second common thread is the near absence of H_2O as a cluster partner in spite of the obvious importance of this moiety in atmospheric chemistry and other aspects of cluster chemistry. For negative ions, only the $CO_3^- \cdot H_2O$ system has been investigated by our group[6] and $CO_3 \cdot (H_2O)_x$, with $x = 1$–3 by Castleman and coworkers.[7] The reason is simple. The negative ion chemistry of water is essentially nonexistent.[8–10] The H_2O^- ion is apparently not bound[11] and larger clusters are not formed in abundance until $x = 11$.[8,9] However, very small amounts of $(H_2O)_x^-$ clusters can be made in hard expansions using Ar carrier gas (x=2, 6, and 7)[10] indicating these species are at least weakly bound.

Positive ion clusters containing H_2O or H_2O^+ as one of the moieties are essentially unknown. In this case it is not a question of stability but of kinetics. The H_2O^+ ion undergoes very rapid[12] proton transfer to form H_3O^+

$$H_2O^+ + H_2O \rightarrow H_3O^+ + OH, \quad (2)$$

$$H_3O^+ + M \rightarrow H_3O^+ \cdot M, \quad (3)$$

 0021-9606/90/205594-11$03.00

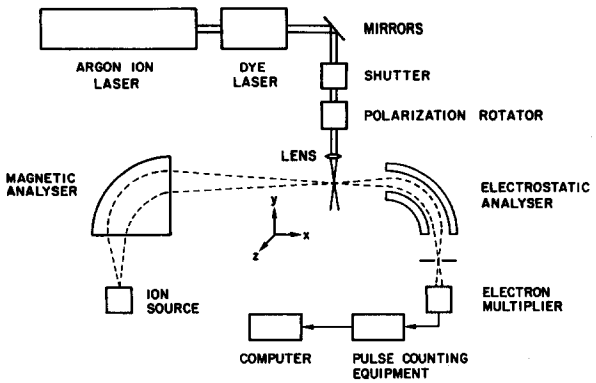

FIG. 1. Schematic diagram of the instrument used in the photodissociation studies.

and H_3O^+ then undergoes rapid clustering with other species present.[13]

In this paper we present our first data on water containing positive ion clusters. We have chosen $Kr \cdot H_2O^+$ as the first system to study because we found we could make this adduct in sufficient quantity and because the Kr moiety, being atomic, would allow the properties of the H_2O^+ ion in the dissociation dynamics to be most fully apparent. The results of our study follow.

II. EXPERIMENTAL

The details of the experimental method have been published previously.[14] A schematic of the instrument is given in Fig. 1. The $Kr \cdot H_2O^+$ cluster was made in a temperature and pressure variable ion source using essentially pure Kr at 0.1 Torr. No H_2O was added. The trace of H_2O present was probably picked up in the inlet line by the Kr gas. The following reactions then took place in the ion source, held at a temperature of 273 K;

$$Kr + e^-(100\ eV) \rightarrow Kr^+ + 2e, \quad (4)$$

$$Kr^+ + H_2O \rightarrow H_2O^+ + Kr, \quad (5)$$

$$H_2O^+ + 2Kr \rightarrow Kr \cdot H_2O^+ + Kr. \quad (6)$$

The charge–transfer reaction (5) is very fast[15] and forms H_2O^+ ions on essentially every collision. The rate for the clustering reaction (6) is not known. The important point is the *rate* of reaction (6) must be much larger than the *rate* of reaction (2). A reasonable value for the third order association, reaction (6), is $1\times10^{-28}\ cm^6\ s^{-1}$. At 0.1 Torr pressure of Kr, the corresponding apparent bimolecular rate constant for reaction (6) is $k_6 \cong 3.3\times10^{-13}\ cm^3\ s^{-1}$. The literature value of k_2 is[12] $k_2 = 2.05\times10^{-9}\ cm^3\ s^{-1}$. Hence, if the *rate* of reaction (6) is to be an order of magnitude greater than the *rate* of reaction (2), $p_{Kr}/p_{H_2O} \geqslant 10k_2/k_6 = 1.5\times10^5$. It follows that for $p_{Kr} = 0.1$ Torr, then $p_{H_2O} \leqslant 1.5\times10^{-6}$ Torr. This low partial pressure of H_2O can only be realized by using totally anhydrous Kr and admitting no H_2O directly into the ion source. The condition is apparently conveniently met simply by allowing Kr to sweep H_2O into the ion source from the walls of the inlet system.

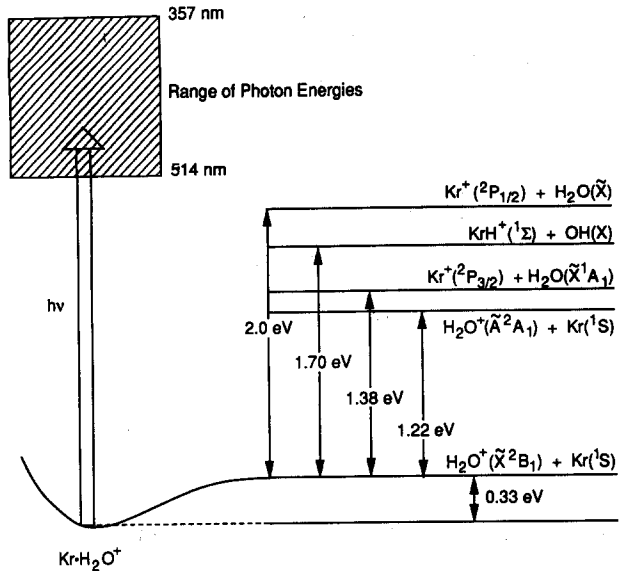

FIG. 2. Schematic diagram showing energy states of importance in this work.

Once the cluster ions are made in the source they drift out the exit slit, are accelerated to 8 kV, and are mass selected by a magnet. The $Kr \cdot H_2O^+$ ions are then brought to a spatial focus and crossed with the output of an argon ion laser where a fraction of the cluster beam is photodissociated. The photoproducts are mass and energy analyzed using a high resolution kinetic energy analyzer and are detected using a venetian blind multiplier.

The output of the argon ion laser is plane polarized. A polarization rotator is inserted into the beam allowing photodissociation spectra to be obtained for polarization angles of 0°, 54.7°, and 90°. Reasons for choosing these angles will be explained later. A shutter is also placed in the laser path. Experiments are done with the laser on and laser off and the difference in the two signals used to identify the pure laser induced signal. This up/down counting process allows subtraction of any background signals due to either natural metastables or collision induced processes.

III. RESULTS

The energetics for the system are summarized in Fig. 2. The energies of the various asymptotic limits are well known from literature data.[16] The binding energy of the $Kr \cdot H_2O^+$ cluster has not been measured. A reasonable estimate of this binding energy is 0.3 ± 0.1 eV based on the fact the ionization potentials of Kr and H_2O are substantially different.[17] Experimental evidence bearing on the value of $D_0^0(Kr\text{–}H_2O^+)$ will be given later in this paper.

A. Photodissociation cross section

The experimental apparatus used for the data to be presented here is not suitable for the measurement of absolute cross sections. However, sometimes it is possible to

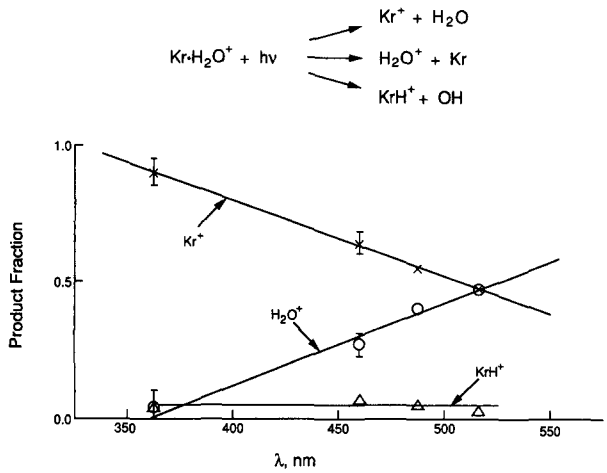

FIG. 3. Product branching ratio for photodissociation of $Kr \cdot H_2O^+$ as a function of wavelength.

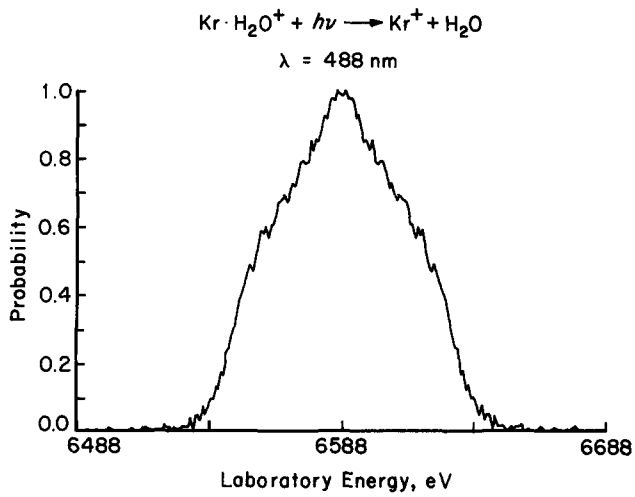

FIG. 4. Laboratory kinetic energy distribution for Kr^+ from photodissociation of $Kr \cdot H_2O^+$ at 488 nm and laser polarization of 54.7°. .

measure photodissociation cross sections relative to measurements made by other methods. The Kr_2^+ dimer coexists in our source with the $Kr \cdot H_2O^+$ cluster. The photodissociation cross section of Kr_2^+ has been measured by Lee and Smith.[18] They obtain a value of 1×10^{-19} cm^2 at 483 nm. We compared the photodissociation cross sections of Kr_2^+ and $Kr \cdot H_2O^+$ at 488 nm and determined $\sigma_{Kr \cdot H_2O^+} \cong 2\sigma_{Kr_2^+}$. Due to signal to noise problems it was not possible to do an accurate study at the other wavelengths we used in this work.

B. Product branching ratios

One of the reasons for studying the water containing clusters is the possibility that intracluster chemical reactivity could be photoinduced. The product branching ratio as a function of wavelength is given in Fig. 3. At 357 nm the Kr^+ ionic photoproduct dominates, making up 91% of the ionic products. As λ increases, the fraction of Kr^+ ionic product decreases until at 514 nm the Kr^+ and H_2O^+ fractions each make up 48% of the products. The KrH^+ ionic product is present at all wavelengths accounting for $\sim$5% of the products independent of λ. Hence, the $Kr \cdot H_2O^+$ cluster acts predominantly like all other clusters we have studied, where the individually clustered moieties retain their identity on photodissociation. The fact that KrH^+/OH products are observed, however, is noteworthy as it is the first time intracluster atom transfer chemistry has been observed in our studies.

The particular electronic states of the photo products are not indicated in Fig. 3. The krypton ion has both Kr^+ ($^2P_{3/2}$,$^2P_{1/2}$) spin states accessible in the energy range studied and the water ion has H_2O^+ (X,A) states accessible. More will be said about these state distributions shortly.

C. Product kinetic energy distributions

As mentioned in Sec. II, photodissociation is done for three separate polarization angles of the laser relative to the ion beam direction; 0°, 54.7°, and 90°. The 54.7° angle is the so-called "magic angle" because at this angle the measured laboratory kinetic energy peak shape of the ionic photoproduct is the same as the peak shape would be for a completely isotropic fragmentation process.[19] The center of mass kinetic energy distribution for the fragmentation can be obtained from the measured laboratory peak using a simple transformation.[20]

1. $Kr^+ + H_2O$ products

The parent cluster ion, $Kr \cdot H_2O^+$, has the charge primarily localized on the H_2O moiety since it takes 1.38 eV more energy to remove an electron from Kr to form Kr^+ ($^2P_{3/2}$) than it does from H_2O to form H_2O^+ ($\tilde{X}\ ^2B_1$). Hence, in this product channel we are observing a photon induced charge–transfer reaction,[21] a process we have studied in some detail previously.[3(a),22,23] The fact that this process is observed, and dominates at short wavelength, is strong evidence for state specific dynamics rather than statistical-type behavior.

A typical laboratory peak for Kr^+/H_2O photoproducts taken at 54.7° at $\lambda = 488$ nm is given in Fig. 4. The rather broad shoulders on this peak and narrow center portion is very suggestive of a bimodal distribution of Kr^+ product ion in the center of mass. These distributions are given in Fig. 5 for 514, 488, 454, and 357±7 nm.

The 514 nm distribution is generally triangular in shape, peaking at 0.33 eV. There is some indication that a small second peak could exist at low values of kinetic energy.

The 488 nm peak is clearly bimodal as suggested by the laboratory peak shape in Fig. 4. The main peak is again triangular in shape and peaks at 0.35 eV. The lower energy peak suggested at 514 nm is now clearly resolved.

At 458 nm there are clearly two components in the kinetic energy distribution. Both are triangular in shape, with the outer component peaking near 0.46 eV and the inner component near 0.14 eV.

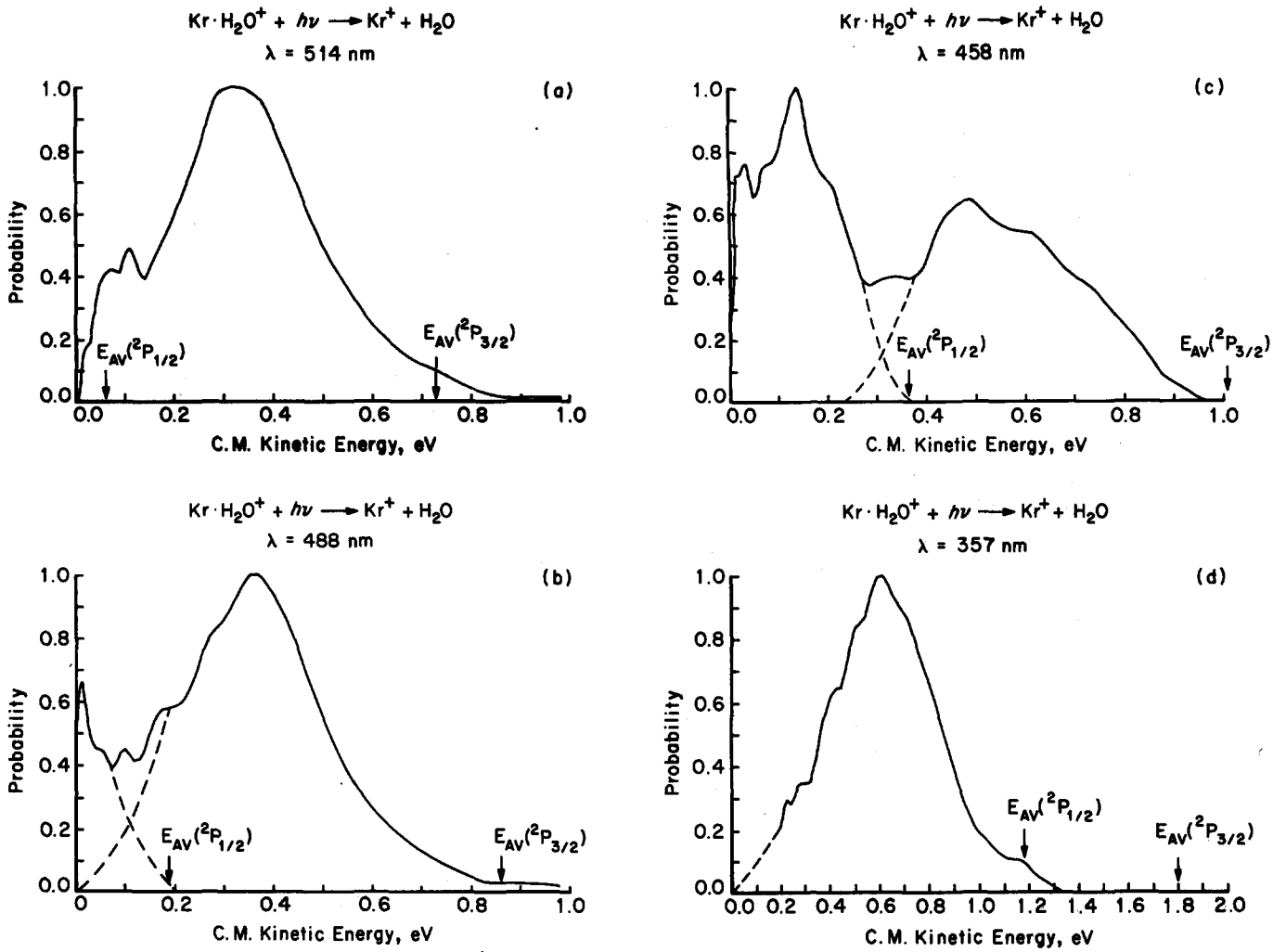

FIG. 5. Center of mass kinetic energy distributions for $Kr^+ + H_2O$ products from photodissociation of $Kr{\cdot}H_2O^+$. The arrows on the horizontal axis denote the maximum amount of energy that can appear as kinetic energy for Kr^+ formed in either the $^2P_{3/2}$ or $^2P_{1/2}$ state. (a) 514 nm, (b) 488 nm, (c) 458 nm, (d) 357±7 nm. Note the energy scale is different in (d).

Finally, at 357±7 eV there is again one component, again triangular in shape and peaking near 0.53 eV. The structure near zero kinetic energy in this peak is noise and is not reproducible.

The shape of each of these distributions is strongly suggestive of a repulsive upper state. The assignment of the peaks and the origin of the structure evident at 488 and 458 nm can be aided by looking at an energy conservation relationship. For the reaction

$$Kr{\cdot}H_2O^+ + h\nu \rightarrow Kr^+(^2P_{3/2},^2P_{1/2}) + H_2O \qquad (7)$$

the energy available to the products is

$$E_{AV} = h\nu - D_0^0(Kr - H_2O^+) - \Delta IP(Kr,H_2O) + E_{int}(Kr{\cdot}H_2O^+), \qquad (8)$$

where $\Delta IP(Kr,H_2O)$ is the difference in ionization energies of Kr and H_2O and $E_{int}(Kr{\cdot}H_2O^+)$ is the internal energy in the $Kr{\cdot}H_2O^+$ cluster that adsorbs the photon. This latter energy is bounded by $D_0^0(Kr{-}H_2O^+) > E_{int}(Kr{\cdot}H_2O^+) > 0$. At typical source pressures (0.1 Torr) and source residence times (50 μs), a typical $Kr{\cdot}H_2O^+$ cluster will experience 100±50 collisions. Hence, $E_{int}(Kr{\cdot}H_2O^+)$ is essentially the thermal value of 0.025 eV.

Arrows indicating E_{AV} for the $Kr^+(^2P_{3/2})$ and $Kr^+(^2P_{1/2})$ product channels are placed on the energy axes in Fig. 5. For 514 nm laser light, $E_{AV}[Kr^+(^2P_{3/2})]$ comes at 0.73 eV which corresponds closely with the high energy onset of the Kr^+/H_2O kinetic energy distribution. In principal the products cannot have kinetic energy above this value. The distribution tails slightly above this value indicating a few percent of the $Kr{\cdot}H_2O^+$ clusters have internal energies as large as 0.1 eV. These clusters were most likely formed very near the source exit slit and did not suffer sufficient collisions to be thermalized.

The value of $E_{AV}[Kr^+(^2P_{1/2})]$ comes at 0.06 eV and places an upper limit on $Kr^+(^2P_{1/2})/H_2O$ products. Clearly a maximum of a few percent of the Kr^+ products are formed in $^2P_{1/2}$ spin state at 514 nm.

The 488 nm data are given in Fig. 5(b). Again the values of E_{AV} are marked for the two Kr^+ spin states. The high energy peak appears to be unambiguously associated with the $Kr^+(^2P_{3/2})$ state. The low energy peak appears to

TABLE I. Branching ratio in the reaction

$$Kr{\cdot}H_2O^2 + h\nu \rightarrow Kr^+(^2P_{3/2}) + H_2O$$
$$Kr{\cdot}H_2O^2 + h\nu \rightarrow Kr^+(^2P_{1/2}) + H_2O$$

	E_{AV} (eV)[a]		Percent	
λ (nm)	$^2P_{3/2}$	$^2P_{1/2}$	($^2P_{3/2}$)	($^2P_{1/2}$)
514	0.73	0.06	~100	~0
488	0.86	0.19	84	16
458	1.03	0.36	55	45
357	1.79	1.12	~0	~100

[a] E_{AV} is the available energy for each reaction channel calculated from Eq. (8) in the text. The uncertainty is ±10%.

be most reasonably associated with the $Kr^+(^2P_{1/2})$ state. In principal it could be due to vibrationally excited H_2O products but almost certainly this is not the case. The kinetic energy distribution from 0.9 to 0.3 eV is smooth and shows no sign of selective vibrational excitation in H_2O. It is not physically reasonable this excitation would suddenly occur nearly 0.9 eV above threshold when H_2O has vibrational frequencies of 0.45, 0.20, and 0.47 eV.

An estimate of the fractions of $Kr^+(^2P_{3/2})$ and $Kr^+(^2P_{1/2})$ in the products can be made by smoothly extrapolating the two distributions as shown by the dashed lines in Fig. 5(b). Such a procedure indicates 84% $Kr^+(^2P_{3/2})$ and 16% $Kr^+(^2P_{1/2})$. This data are summarized in Table I.

The 458 nm data are given in Fig. 5(c), along with the specifications of E_{AV} for both $^2P_{3/2}$ and $^2P_{1/2}$ of Kr^+. Here the bimodality is very obvious and it is clear that no combination of H_2O vibrational excitation can explain the gross structure. Smooth extrapolations of the two components allow estimates of 55% $^2P_{3/2}$ and 45% $^2P_{1/2}$ to be made.

Finally, the 357±7 nm data are given in Fig. 5(d), along with markers for E_{AV}. Only a single peak is observed, apparently corresponding to pure $Kr^+(^2P_{1/2})$ product. Again it appears obvious that vibrational excitation of H_2O does not play a big role in the dynamics.

2. H_2O^+ + Kr products

The laboratory H_2O^+ product ion peak is given in Fig. 6(a) for 488 nm photons. The shape is smooth with no apparent shoulders that suggest structure in the kinetic energy distribution. This suggestion is confirmed in the center of mass kinetic energy release distribution given in Fig. 6(b). The distribution peaks at very low energy and falls off quasiexponentially to higher energy. This shape is suggestive of a vibrational predissociation mechanism from a bound state. Two possible product states are energetically feasible:

$$Kr{\cdot}H_2O^+ + h\nu \rightarrow H_2O^+(\tilde{X}\ ^2B_1) + Kr \quad (9a)$$
$$Kr{\cdot}H_2O^+ + h\nu \rightarrow H_2O^+(\tilde{A}\ ^1A_1) + Kr. \quad (9b)$$

These differ in energy by 1.22 eV (see Fig. 2). Hence, the fact that a simple kinetic energy distribution is observed,

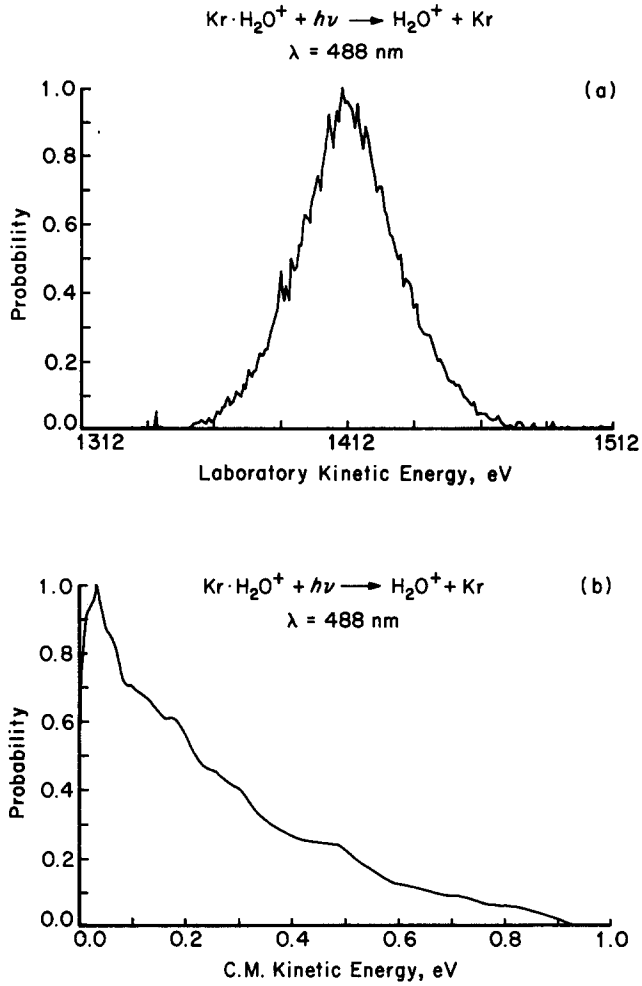

FIG. 6. Photodissociation of $Kr{\cdot}H_2O^+$ to give H_2O^+ + Kr at 488 nm and laser polarization of 54.7°. (a) Laboratory kinetic energy distribution. (b) Center of mass kinetic energy distribution of the products.

with no hint of bimodality, suggests that nearly pure $H_2O^+(\tilde{X}\ ^2B_1)$ or $H_2O^+(\tilde{A}\ ^1A_1)$ product ions are formed. This question will be addressed further in Sec. IV.

Similar distributions to those reported in Fig. 6 are also observed at 514, 458, and 357±7 nm wavelengths. Consequently, it can be said with some confidence that the upper state(s) responsible for the H_2O^+/Kr products are almost certainly different from the state(s) responsible for Kr^+/H_2O products and these states do not communicate once they have formed.

3. KrH^+ + OH products

The KrH^+ + OH products are very minor at every wavelength. Since the total cross section for photodestruction of $Kr{\cdot}H_2O^+$ is about 2×10^{-19} cm^2, the KrH^+/OH channel has a cross section around 1×10^{-20} cm^2. Hence, relatively accurate product energy distributions could only be obtained for the stronger laser lines at 488 and 514 nm. The center of mass kinetic energy distribution at 488 nm is given in Fig. 7. This distribution is similar in shape to that found for H_2O^+/Kr products and suggests vibrational predissociation from a bound state as the dissociation mechanism. More will be said about this process in Sec. IV.

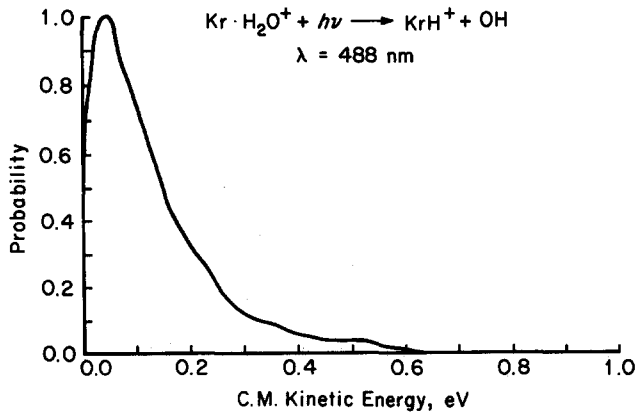

FIG. 7. Center of mass kinetic energy distribution for $KrH^+ + OH$ products from $Kr{\cdot}H_2O^+$ at 488 nm.

D. Product angular distributions

In general, a photodissociation event does not lead to an isotropic distribution of products, even if the photoexcited cluster is relatively long lived. A useful model treats the dissociating products as quasiatomic species whose spatial distribution will be determined primarily by the properties of the dissociation coordinate and not by other motions within either of the fragment moieties. This is a relatively good approximation for the $Kr{\cdot}H_2O^+$ system because the products are either atoms or simple, strongly bound molecules. In this limit, the angular distribution of the products is given by[24]

$$P(\theta)=(4\pi)^{-1}[1+\beta P_2(\cos\theta)], \tag{10}$$

where $P(\theta)$ is the probability that the products fragment into a solid angle $d\omega$ at an angle θ with respect to the laser electric vector, $P_2(\cos\theta)$ is the second degree Legendre polynomial in $\cos\theta$, and β is the so-called "asymmetry parameter" that characterizes the degree of anisotropy in the fragment angular distribution. In general, $-1\leqslant\beta\leqslant 2$ for all reactions and $0\leqslant\beta\leqslant 2$ for parallel transitions between the transition dipole and the dissociation axis. Considering parallel transitions only,[25] $0\leqslant\beta\leqslant 0.5$ for processes where the photoexcited state lives longer than a rotational period and $0.5\leqslant\beta\leqslant 2$ for systems living shorter than a rotational period.

In our experiment the greatest demonstration of anisotropy in the product angular distribution occurs by comparing the laboratory peak shapes for laser polarizations of 0° and 90° with respect to the ion beam direction. We have developed methods for extracting asymmetry parameters from comparison of these peak shapes.[26] These methods were extended[27] to obtain microscopic values of $\beta(E_t)$ for each value of the product translational energy distribution. Both average values[26] and microscopic values[27] have importance as we will see.

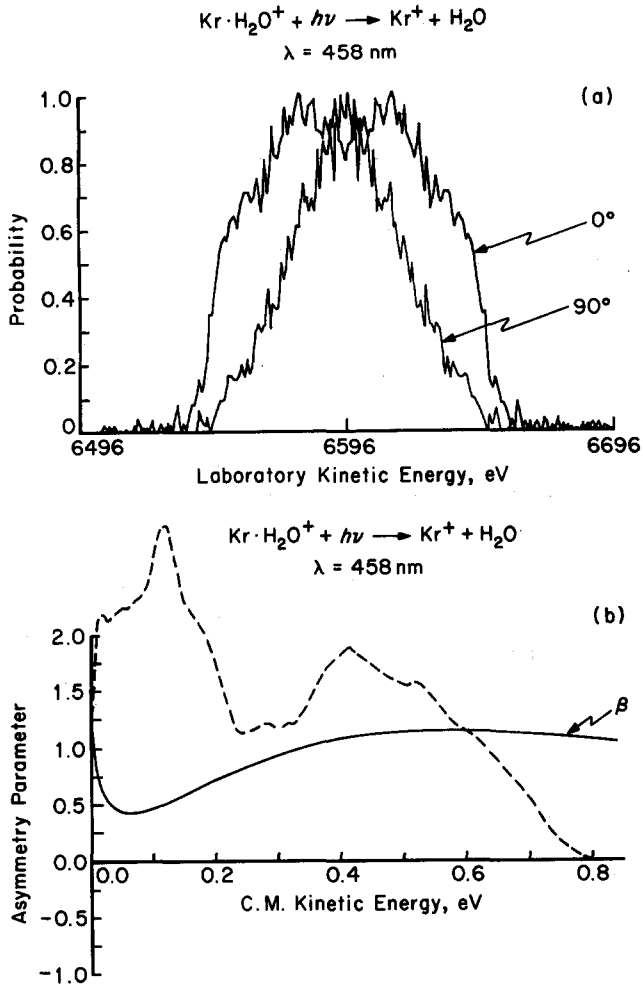

FIG. 8. Photodissociation of $Kr{\cdot}H_2O^+$ to give $Kr^+ + H_2O$. (a) Laboratory kinetic energy distributions for laser polarizations of 0° and 90°. (b) A plot of the asymmetry parameter β vs product kinetic energy. The center of mass kinetic energy distribution of the $Kr^+ + H_2O$ products is shown for reference as the dashed line.

1. $Kr^+ + H_2O$ products

The laboratory peaks for laser polarization angles of 0° and 90° are given in Fig. 8 (a) for $\lambda = 458$ nm. The 90° peak is clearly much narrower than the 0° peak indicating the upper state must be short lived relative to a rotational period. The 0° peak is also slightly bimodal, a further indication of a repulsive upper state. The asymmetry parameter analysis of these peak shapes is given in Fig. 8(b). The value of β exceeds 0.5 for virtually the entire range of product kinetic energies, indicating an upper state(s) whose dissociative lifetime is much shorter than a rotational period. By comparing $\beta(E_t)$ with the kinetic energy distribution given in Fig. 5, an average value of $\bar{\beta}$ can be obtained for both $Kr^+(^2P_{1/2})$ and $Kr^+(^2P_{3/2})$ products. These values are given in Table II for all accessible wavelengths.

2. $H_2O^+ + Kr$ products

The laboratory peaks for 0° and 90° laser polarization for H_2O^+/Kr products are given in Fig. 9 (a) for $\lambda = 514$ nm. The 0° peak is only slightly broader than the 90° peak

TABLE II. Average product kinetic energies and asymmetry parameters for the reactions.

$$Kr\cdot H_2O^+ + h\nu \rightarrow \begin{cases} Kr^+(^2P_{3/2},^2P_{1/2}) + H_2O \\ H_2O^+ + Kr \\ KrH^+ + OH. \end{cases}$$

	$Kr^+(^2P_{3/2})$			$Kr^+(^2P_{1/2})$			H_2O^+			KrH^+		
λ (nm)	E_{AV}[a]	$\bar{E}_t$[a]	$\bar{\beta}$	E_{AV}[a]	$\bar{E}_t$[a]	$\bar{\beta}$	E_{AV}[a,b]	$\bar{E}_t$[a]	$\bar{\beta}$	E_{AV}[a]	$\bar{E}_t$[a]	$\bar{\beta}$
514	0.06	~0	···	0.73	0.35	0.8	0.89	0.25	0.4	0.41	0.12	0.3
488	0.19	0.07	0.25	0.86	0.38	0.9	1.02	0.26	0.4	0.54	0.13	0.3
458	0.36	0.16	0.65	1.03	0.55	1.1	1.18	0.26	···	0.71	···	···

[a]In eV. While these numbers are quoted to two significant figures, there is an uncertainty in E_{AV} of $\pm 10\%$.
[b]Assumes $H_2O^+(\tilde{A}\,^2A_1)$ product. Add 1.22 eV for $H_2O^+(\tilde{X}\,^2B_1)$.

indicating significant rotational averaging has occurred before dissociation. This conclusion is confirmed by the asymmetry parameter analysis given in Fig. 9(b), where $\beta(E_t) \cong 0.4$ over the entire product kinetic energy range of interest. These results are entirely consistent with the kinetic energy distribution data in Fig. 6 that suggested a vibrational predissociation mechanism may be responsible for this product channel. The data are summarized in Table II.

3. $KrH^+ + OH$ products

The signal to noise in this channel was quite poor at all wavelengths. Nonetheless, we were able to show that the 0° and 90° peak shapes were very similar at $\lambda = 514$ and 488 nm and average values $\bar{\beta} = 0.3 \pm 0.1$ were obtained. These results indicate substantial rotational averaging has occurred before dissociation, a result consistent with the kinetic energy release measurements. The data are summarized in Table II.

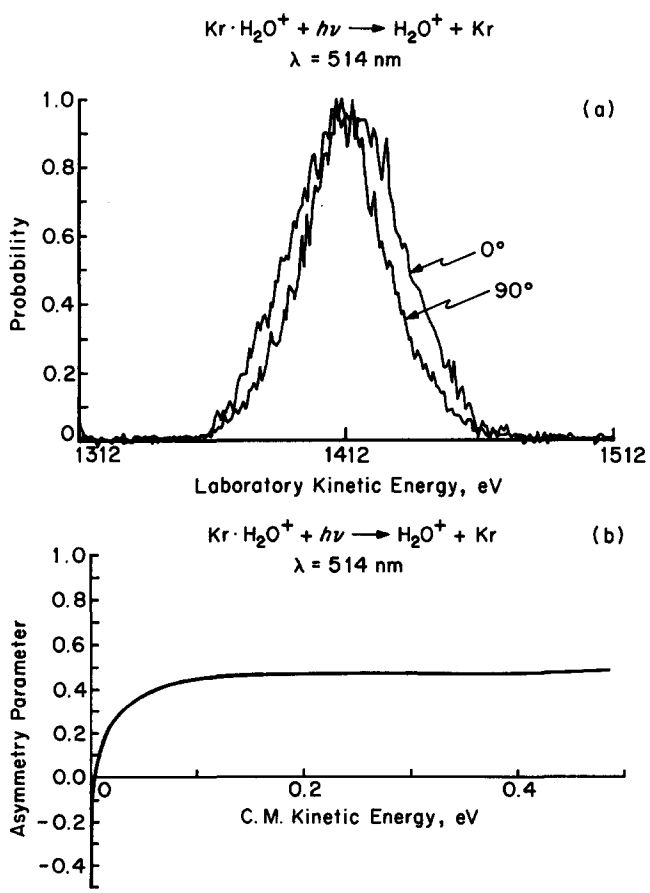

FIG. 9. Photodissociation of $Kr\cdot H_2O^+$ to give H_2O^+ + Kr. (a) Laboratory kinetic energy distributions for laser polarizations of 0° and 90°. (b) A plot of the asymmetry parameter β vs center of mass kinetic energy.

IV. DISCUSSION

One immediately apparent conclusion that can be made is that the upper states leading to Kr^+/H_2O products and to H_2O^+/Kr products are completely different in character and these states do not communicate before dissociation to products occurs. The Kr^+ product ions result from direct dissociation from a repulsive state that is very short lived while the H_2O^+ ions are formed from much longer lived cluster states. The KrH^+/OH ions also fall into this latter category. The branching ratios reported in Fig. 2 reflect, then, the Franck–Condon factors for accessing these various upper states as λ varies from 357 ± 7 to 514 nm. As λ increases the state(s) leading to H_2O^+ formation become more accessible. The KrH^+/OH branching ratio is independent of λ, indicating these products may not come from the same bound upper state(s) that lead to H_2O^+ formation.

Since the major products Kr^+/H_2O and H_2O^+/Kr are formed from upper states that are isolated from each other, the two product channels will be discussed separately.

A. $Kr^+ + H_2O$ products

All of the evidence indicates these products arise from repulsive upper states that lead directly to either $Kr^+(^2P_{1/2})/H_2O(\tilde{X})$ or $Kr^+(^2P_{3/2})/H_2O(\tilde{X})$. In the past we have been able to successfully apply[4] an impulsive model[28] to obtain some information on the structure of the ground state of the cluster before it absorbs the photon. The idea is that since the photo excited state dissociates instantly, the repulsive force will be felt primarily by the atoms making up the "bond" being broken. This analysis yields the relationship given by

$$\frac{\Delta \bar{E}_t}{\Delta E_{AV}} = \frac{\mu_{BC}}{\mu_F}, \tag{11}$$

where B and C are the atoms in the breaking bond, μ_{BC} is their reduced mass, and μ_F is the reduced mass of the

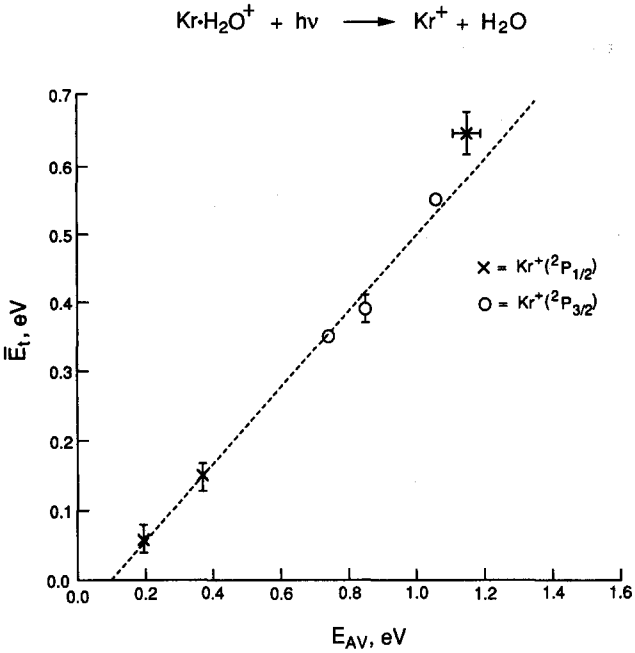

FIG. 10. A plot of the average product kinetic energy E_t vs the available energy E_{AV} for photodissociation of $Kr \cdot H_2O^+$ to give $Kr^+ + H_2O$. Typical error bars are shown.

photofragments (in this case Kr^+ and H_2O). A plot of $\overline{E}_t$ vs E_{AV} is given in Fig. 10 . A linear relationship is observed over a very broad energy range with a slope $\Delta\overline{E}_t/\Delta E_{AV} = 0.53 \pm 0.1$. This can be compared with slopes predicted from various structures

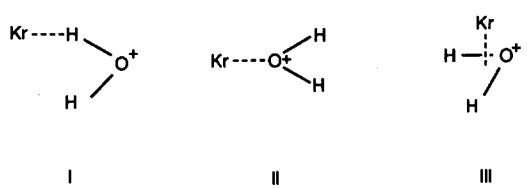

For structure I, $\mu_{BC}/\mu_F = 0.07$ and for structure II, $\mu_{BC}/\mu_F = 0.91$. Clearly neither of these limiting cases can represent the true structure and hence the Kr atom is not bound to either an H atom or O atom in the cluster ground state. In order to obtain a match with experiment, a reduced mass of 8.6 ± 1.6 is indicated for μ_{BC}. Hence, the Kr atom is associated with one or both of the O–H bonds. One possible structure is given in structure III, although many such structures can be drawn with the Kr atom either in or out of the plane of the H_2O molecule. More will be said about this point later.

Additional information can be obtained by rearranging Eq. (8) and using the kinetic energy release data in Fig. 5,

$$h\nu - \Delta IP(Kr,H_2O) - \overline{E}_t(Kr^+/H_2O)$$
$$= D_0^0(Kr\text{–}H_2O^+) + \overline{E}_{int}(H_2O) + \overline{E}_{int}(Kr), \quad (12)$$

where we have noted that the available energy for product formation must appear as either translational or internal energy in the products; i.e., $E_{AV} = \overline{E}_t(Kr^+/H_2O) + \overline{E}_{int}(H_2O) + \overline{E}_{int}(Kr)$. In Eq. (12) we have eliminated the term $\overline{E}_{int}(Kr \cdot H_2O^+)$ since this is small

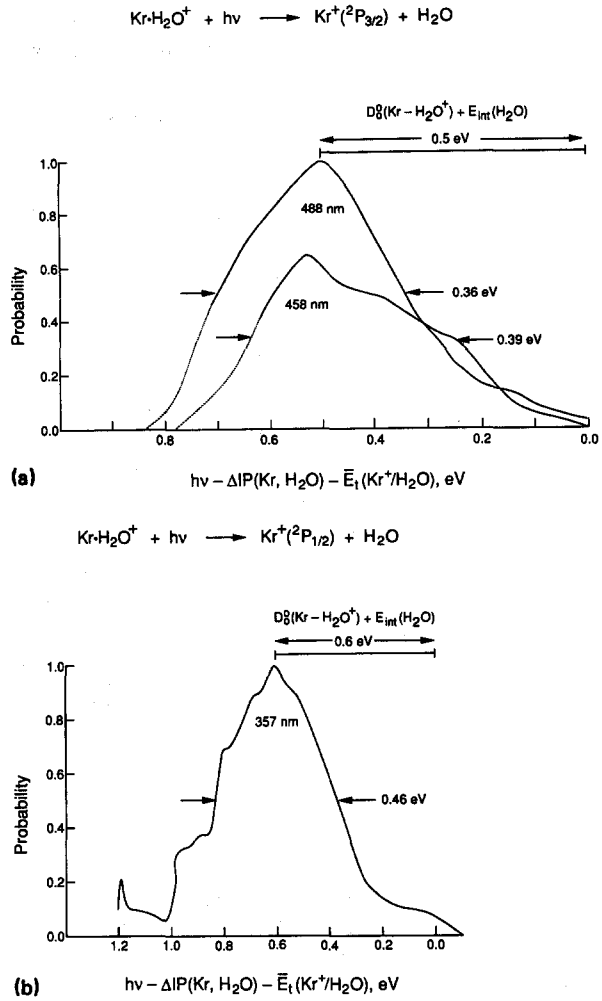

FIG. 11. A plot of $h\nu - \Delta IP(Kr,H_2O) - \overline{E}_t(Kr^+,H_2O)$ for center of mass kinetic energy distributions of products of the photodissociation of $Kr \cdot H_2O^+$ to give $Kr^+ + H_2O$: (a) For 488 and 458 nm; (b) 357 ± 7 nm (see the text).

($\sim$0.025 eV). Also note that $\overline{E}_{int}(Kr) = 0$ is an excellent approximation since no excited states are energetically accessible. Portions of the kinetic energy release data in Fig. 5 are reported in Fig. 11 using a coordinate system defined by Eq. (12).

Consider first the 458 and 488 nm data in Fig. 11(a). According to Eq. (12) the average energies of the peak maxima $\overline{E}_{pm}$ are given by

$$\overline{E}_{pm} = D_0^0(Kr\text{–}H_2O^+) + \overline{E}_{int}(H_2O). \quad (13)$$

The shapes of the peaks are due to the internal energy distributions in the products. To a good first approximation the half-widths at half-height of the peaks are the average internal energy in the water molecule fragment. From the figure, $\overline{E}_{int}(H_2O) = 0.18$ eV at 488 nm and 0.19 eV at 458 nm with an uncertainty of ± 0.05 eV. Consequently,

$$D_0^0(Kr\text{–}H_2O^+) \cong \overline{E}_{pm} - \overline{E}_{int}(H_2O),$$

where $\overline{E}_{pm}$ is 0.5 ± 0.05 eV at both wavelengths giving bond dissociation energies of 0.3 ± 0.1 for both the 488 and 458 nm data. This is a very reasonable result based on

analogy to measured bond energies in similar clusters where the ionization potentials of the two partners are very different.[3(a)]

The data for $\lambda = 357 \pm 7$ nm are given in Fig. 11(b). In this instance $\overline{E}_{pm} = 0.6 \pm 0.05$ eV and $\overline{E}_{int}(H_2O) = 0.23 \pm 0.05$ eV giving $D_0^0(Kr\text{–}H_2O^+) = 0.37 \pm 0.1$ eV in reasonably good agreement with the 458 and 488 nm data. This is important because at 357 nm $Kr^+(^2P_{1/2})$ is the exclusive product while at 458 and 488 nm both $Kr^+(^2P_{1/2},^2P_{3/2})$ products are formed but $Kr^+(^2P_{3/2})$ data were used due to uncertainty in the exact centers and widths of the $Kr^+(^2P_{1/2})$ peaks.

The peak widths are almost certainly due to rotational excitation in the H_2O photoproduct since the vibrational states in H_2O are so widely spaced (0.45, 0.2, and 0.47 eV) and structure would be evident if vibrational excitation of H_2O were significant. A rotational energy of 0.2 ± 0.05 eV in H_2O is very large indicating the structure of the $Kr \cdot H_2O^+$ complex must allow large torque in the H_2O fragment during the impulsive dissociation on the repulsive surface. Consequently, "symmetric" in-plane structures such as structure II, or a structure where Kr symmetrically interacts in plane with both H atoms, cannot be involved. This conclusion is in line with deductions made earlier based on how the kinetic energy of the fragments varied with E_{AV}. In fact, the very large rotational excitation of H_2O supports an out of plane structure, like III, where a maximum torque can be applied to the departing H_2O fragment. More precise structural information on $Kr \cdot H_2O^+$ awaits good *ab initio* calculations or spectroscopic experiments.

B. $H_2O^+ + Kr$ products

The H_2O^+/Kr products have characteristics consistent with a photon accessing a bound upper state followed by vibrational predissociation. As indicated in Fig. 2 and Eq. (9), either of two water ion products are energetically possible: $H_2O^+(\tilde{X}\ ^2B_1)$ or $H_2O^+(\tilde{A}\ ^2A_1)$. The product kinetic energy distribution [Fig. 6(b)] peaks at low energy and falls essentially exponentially to zero. In the past[4] we have successfully modeled data such as these using statistical phase space theory.[28] The details of the calculations have been extensively discussed elsewhere.[29]

The results of the calculations are plotted in Fig. 12 for $\lambda = 514$ nm. Calculations are given for both ground state $H_2O^+(\tilde{X}\ ^2B_1)$ and electronically excited $H_2O^+(\tilde{A}\ ^2A_1)$ products. Clearly the calculation assuming ground state $H_2O^+(\tilde{X}\ ^2B_1)$ products is much broader than observed experimentally. On the other hand, the calculation assuming $H_2O^+(\tilde{A}\ ^2A_1)$ products fits experiment essentially exactly. This fit provides very strong evidence that the water ion fragment is formed strongly internally excited via a vibrational predissociation mechanism. Whether this fragment is actually formed in the $\tilde{A}\ ^2A_1$ state or is vibrationally excited $\tilde{X}\ ^2B_1$ will be discussed next.

Two aspects of the current system make it especially interesting. First H_2O^+ is formed with ~ 1.22 eV internal energy, perhaps as pure $\tilde{A}\ ^2A_1$. This result is observed at both 488 and 514 nm. Second, the photon is absorbed at

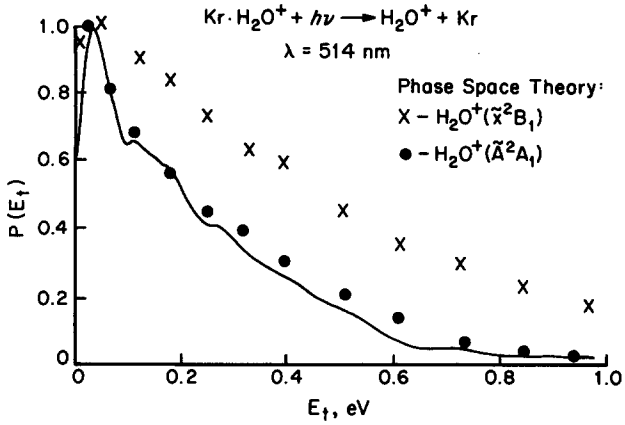

FIG. 12. Product center of mass kinetic energy distribution for photodissociation of $Kr \cdot H_2O^+$ to give $H_2O^+ + Kr$. The phase space theory results for $H_2O^+(\tilde{A}\ ^2A_1)$, plotted as the filled circles, actually represent calculations where 1.3 eV is subtracted from the available energy assuming ground state products. See the text.

energies 0.7 to 0.9 eV above the $H_2O^+(\tilde{A}\ ^2A_1)/Kr$ dissociation asymptote. Hence, direct absorption into a bound state directly correlating to $H_2O^+(\tilde{A}\ ^2A_1)$ is expected to have very small Franck–Condon factors, at least for motions strongly coupled to the dissociation axis, since the wave function for these vibrational states is so diffuse. Consequently, if $H_2O^+(\tilde{A}\ ^2A_1)$ is formed, either a second bound state is involved that absorbs the photon followed by internal conversion to the bound state correlating to $H_2O^+(\tilde{A}\ ^2A_1)/Kr$ and vibrational predissociation, or absorption occurs directly to the bound state correlating to $H_2O^+(\tilde{A}\ ^2A_1)/Kr$ products but in vibrational coordinates only weakly coupled to the dissociation axis. If the former occurs, the question becomes why did the system not prefer to internally convert to the ground state, since the density of states of the ground state is much higher at the energies involved?

In the past[4] we have often argued that the photon is absorbed by "cluster states" rather than states isolated on any of the cluster moieties. This is certainly true for repulsive states where products containing only cluster moieties are formed. Such states are almost certainly involved in formation of the Kr^+/H_2O products discussed earlier. In the case of $CO_3^- \cdot X$, for $X = H_2O$ or CO_2, however, the photon was initially absorbed by the CO_3^- chromophore.[6] The evidence is not quite as convincing for the $Kr \cdot SO_2^+$ dimer[30] or $(SO_2)_3^+$ trimer,[31] but in both cases SO_2^+ may be the chromophore for a fraction of the products formed. There are two SO_2^+ excited states energetically accessible: the $\tilde{A}\ ^2A_2$ state at 0.71 eV and the $\tilde{B}\ ^2B_1$ state at 0.94 eV.

In the $Kr \cdot H_2O^+$ system a possible dissociation mechanism could be

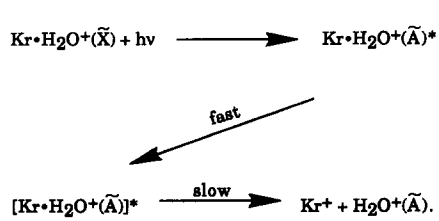

(14)

In Eq. (14), $Kr \cdot H_2O^+(\tilde{A})^*$ indicates the energy is localized on $H_2O^+(\tilde{A})$ while $[Kr \cdot H_2O(\tilde{A})]^*$ indicates the energy is delocalized on the entire $Kr \cdot H_2O^+$ cluster. A key point of this mechanism is the intramolecular energy transfer step from $Kr \cdot H_2O^+(\tilde{A})^* \rightarrow [Kr \cdot H_2O^+(\tilde{A})]^*$ is much faster than the subsequent dissociation of $[Kr \cdot H_2O^+(\tilde{A})]^*$. It is not obvious that this is a reasonable assumption.

An alternative is the mechanism

$$\begin{array}{ccc} Kr{\bullet}H_2O^+(\tilde{X}) + h\nu & \longrightarrow & Kr{\bullet}H_2O^+(\tilde{Z})^* \\ & \swarrow \text{fast} & \\ Kr{\bullet}H_2O^+(\tilde{X})^{**} & \xrightarrow{\text{slow}} & [Kr{\bullet}H_2O^+(\tilde{X})^*]^* \\ & \swarrow \text{fast} & \\ Kr + H_2O^+(\tilde{X})^*. & & \end{array} \tag{15}$$

In this mechanism internal conversion of a bound excited state $H_2O^+(\tilde{Z})^*$ to the highly vibrationally excited ground state, $H_2O^+(\tilde{X})^{**}$, occurs rapidly followed by slow intramolecular energy transfer of *some* of the vibrational energy of $H_2O^+(\tilde{X})^{**}$ to the global cluster modes. Once several vibrational quanta have been transferred the system can dissociate and the competition between the intramolecular energy transfer rate and the dissociation rate determines how much vibrational energy is left in $H_2O^+(\tilde{X})^*$ when dissociation occurs. This is essentially the model used for the $CO_3^- \cdot H_2O$ and $CO_3^- \cdot CO_2$ systems.[6] It is appealing because each of the processes is reasonable and there is precedent for the mechanism in the literature.[6] The major problem with this mechanism is it would require, fortuitously, that $H_2O^+(\tilde{X})^*$ have precisely 1.22 eV of vibrational energy, i.e., the same internal energy as $H_2O^+(\tilde{A})$, since the phase space theory calculations fit experiment assuming $H_2O^+(\tilde{A})$ products. This is a very unlikely circumstance, especially when one considers this internal energy does not change when the photon energy changes from 2.41 to 2.53 eV (514 to 488 nm).

In our view both mechanisms (14) and (15) are plausible but both have aspects that bring them into question. At this point a clear distinction between the two cannot be made with the data in hand.

C. $KrH^+ + OH$ products

One of the goals of this research was to investigate photon induced intracluster chemistry. Partial achievement of this goal occurred because KrH^+/OH products were observed. However, the fact that only 5% of the products ended up in this reaction channel was disappointing. The product kinetic energy release distribution has the shape appropriate for vibrational predissociation from a bound state. Consequently, statistical phase space theory was applied and the results given in Fig. 13 for $\lambda = 514$ nm. In the calculations it was assumed that the photoexcited state had internally converted to the ground state before dissociation occurred. The agreement between experiment and theory is good considering the low signal to noise of the experiment.

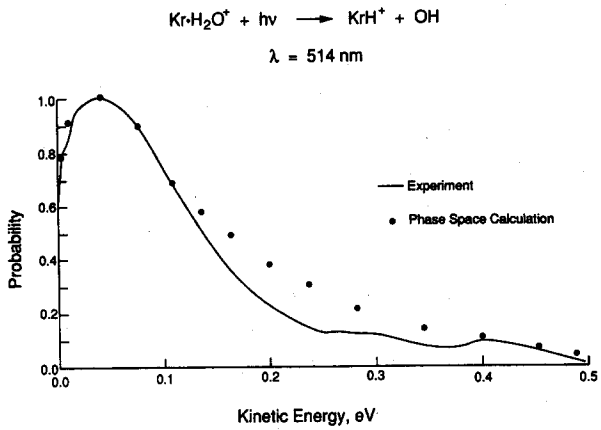

FIG. 13. Product center of mass kinetic energy distribution for photodissociation of $Kr \cdot H_2O^+$ to give $KrH^+ + OH$. The phase space theory results assume all of the available energy is statistically distributed in the products.

This is a puzzling result. If $(Kr \cdot H_2O^+)^{**}$ vibrationally predissociates then $H_2O^+(\tilde{X}) + Kr$ products will overwhelmingly dominate $KrH^+ + OH$ products since they are so much more stable. Yet, the ratio H_2O^+/KrH^+ varies from ~ 1.0 at 357 nm to ~ 10 at 514 nm. Clearly these two products *cannot* be formed by competitive statistical vibrational predissociation of a $(Kr \cdot H_2O^+)^{**}$ complex. Yet, in order to fit the KrH^+/OH kinetic energy release distribution using phase space theory the entire amount of available energy is needed.

A possible mechanism for KrH^+/OH formation is proton or H-atom transfer during dissociation of photoactivated $Kr \cdot H_2O^+$. For example,

$$Kr \cdot H_2O^+ + h\nu \rightarrow [Kr^+ \cdot H_2O]^* \rightarrow Kr^+ + H_2O \tag{16a}$$

$$\downarrow$$

$$[KrH^+ \text{---} OH]^* \rightarrow KrH^+ + OH \tag{16b}$$

if a repulsive charge–transfer state of the complex is accessed then either Kr^+/H_2O products are immediately formed (usual process) or an ion–dipole complex between KrH^+ and OH is formed which subsequently dissociates to KrH^+ and Oh. Formation of this complex, even briefly, could account for the observed asymmetry parameter of 0.3 that indicates substantial rotational averaging has occurred and possibly account for the apparent statistical distribution of energy in the products. The much lower energy products, $H_2O^+(\tilde{X})/Kr$, would, apparently, not be formed since the states involved would correlate only to Kr^+/H_2O or KrH^+/OH. While this is not an entirely satisfactory explanation, it is the best available with the data in hand.

V. CONCLUSIONS

The $Kr \cdot H_2O^+$ cluster photodissociation has been studied from 357 to 514 nm. The principal conclusions of this work are summarized below.

(1) Three ionic products are observed: Kr^+, H_2O^+, and KrH^+. The branching ratio varies strongly with wavelength with Kr^+ dominating at 357 nm (90%) but Kr^+ and H_2O^+ equivalent at 514 nm. The KrH^+ product remains at about 5% independent of λ.

(2) The Kr^+/H_2O products are formed by photoaccessing a repulsive state that directly correlates to these products. Both $Kr^+(^2P_{3/2},^2P_{1/2})$ products are observed and the branching ratio measured as a function of wavelength. Strong variations in the branching ratio are observed with $Kr^+(^2P_{3/2})$ dominating ($\sim 100\%$) at 514 nm and $Kr^+(^2P_{1/2})$ dominating ($\sim 100\%$) at 357 nm.

(3) The H_2O neutral product is strongly rotationally excited. This observation, along with application of an impulsive model to product kinetic energy, indicates the Kr atom in the $Kr \cdot H_2O^+$ cluster is almost certainly located above (or below) the H_2O^+ plane, nearer to the O end of H_2O^+ than the H_2 end.

(5) Energy conservation arguments are used to deduce that $D_0^0(Kr\text{–}H_2O^+) = 0.33 \pm 0.1$ eV.

(6) The H_2O^+/Kr products are formed by statistical vibrational predissociation of a bound state. Phase space theory modeling is consistent with the H_2O^+ product formed either exclusively in $H_2O^+(\tilde{A}\ ^2A_1)$ or in $H_2O^+(\tilde{X}\ ^2B_1)$ with 1.22 eV of vibrational energy. Pros and cons of both possibilities are discussed.

(7) The KrH^+/OH products are also, apparently, formed by vibrational predissociation of a bound state. Arguments are made these products may come from an ion–dipole complex $(KrH^+ \cdot OH)^*$. This is the first observation of photon induced proton transfer in small cluster ions.

ACKNOWLEDGMENTS

This research was supported by the Air Force Office of Scientific Research, Grant No. AFOSR89-0102 and the National Science Foundation, Grant No. CHE88-17201.

[1] D. Smith and N. G. Adams, Top. Curr. Chem. **1**, 89 (1980); E. E. Ferguson, F. C. Fehsenfeld, and D. L. Albritton, in *Gas Phase Ion Chemistry*, edited by M. T. Bowers (Academic, New York, 1979), Vol. 1, p. 45.

[2] A. W. Castleman, Adv. Colloid Interface Sci. **10**, 73 (1979); A. W. Castleman, P. M. Holland, and R. G. Keesee, J. Chem. Phys. **68**, 1760 (1978); J. Heicklen, *Colloid Formation and Growth. A Chemical Kinetics Approach* (Academic, New York, 1976).

[3] (a) M. F. Jarrold, L. Misev, and M. T. Bowers, J. Chem. Phys. **81**, 4369 (1984); (b) See also R. G. Keesee and A. W. Castleman, J. Phys. Chem. Ref. Data **15**, 1011 (1986).

[4] For a recent review, see chapter by M. T. Bowers, in *Ion and Cluster-Ion Spectroscopy and Structure*, edited by J. P. Maier (Elsevier, Amsterdam, 1989), pp. 241–275.

[5] The one certain exception where the photon was absorbed by one of the cluster moieties was in $CO_3^- \cdot X$ systems, where X is H_2O or CO_2. In these cases CO_3^- was the chromophore (Ref. 6).

[6] J. Snodgrass, H-S. Kim, and M. T. Bowers, J. Chem. Phys. **88**, 3072 (1988).

[7] D. E. Hunton, M. Hoffman, T. G. Lindemann, C. R. Albertoni, and A. W. Castleman, Jr., J. Chem. Phys. **82**, 134 (1985).

[8] H. Haberland, C. Ludewigt, H-G. Shirdler, and D. R. Worsnap, Surf. Sci. **156**, 157 (1985); H. Haberland, H. Langosch, H-G. Schirdler, and D. R. Worsnap, J. Phys. Chem. **88**, 3903 (1984).

[9] M. Knapp, O. Echt, D. Kreisle, and E. Ricknagel, J. Phys. Chem. **91**, 2601 (1987).

[10] K. H. Bowen and J. G. Eaton (private communication).

[11] D. M. Chipman, J. Phys. Chem. **82**, 1080 (1978); K. D. Jordan and J. J. Wendoloski, J. Chem. Phys. **21**, 145 (1977); O. H. Crawford and W. R. Garrelty, *ibid.* **66**, 4968 (1977).

[12] W. T. Huntress and R. F. Pinezzotto, J. Chem. Phys. **59**, 4742 (1973); R. C. Bolden and N. D. Twiddy, Faraday Discuss. **53**, 192 (1972).

[13] R. G. Keesee and A. W. Castleman, Jr., J. Phys. Chem. Ref. Data **15**, 1011 (1986).

[14] M. F. Jarrold, A. J. Illies, and M. T. Bowers, J. Chem. Phys. **79**, 6086 (1983); **81**, 214 (1984).

[15] C. J. Howard, H. W. Rundle, and F. Kaufman, J. Chem. Phys. **53**, 3745 (1970); R. Marx, G. Mauclaire, and R. Derai, Int. J. Mass Spectrom. Ion Phys. **47**, 155 (1983).

[16] S. G. Lias, J. E. Bartmess, J. F. Liebman, J. L. Holmes, R. D. Levin, and W. G. Mollard, J. Phys. Chem. Ref. Data **17** (1988), supplement 1.

[17] For a comparison with similar systems and a discussion see the first citation in Ref. 3 of this paper.

[18] L. C. Lee and G. P. Smith, Phys. Rev. A **19**, 2329 (1979).

[19] M. F. Jarrold, A. J. Illies, and M. T. Bowers, J. Chem. Phys. **81**, 214 (1984).

[20] M. F. Jarrold, A. J. Illies, N. J. Kirchner, W. Wagner-Redeker, M. T. Bowers, M. L. Mandich, and J. L. Beauchamp, J. Phys. Chem. **87**, 2213 (1983).

[21] Such a process was first identified by R. A. Beyer and J. A. Vanderhoff, J. Chem. Phys. **65**, 2313 (1976). Detailed dynamical studies were first reported for photoinduced charge–transfer half-collision in Refs. 3(a), 22, and 23.

[22] A. J. Illies, M. F. Jarrold, W. Wagner-Redeker, and M. T. Bowers, J. Am. Chem. Soc. **107**, 2842 (1985).

[23] H-S. Kim, C-H. Kuo, and M. T. Bowers, J. Chem. Phys. **87**, 2667 (1987).

[24] R. N. Zare, Mol. Photochem. **4**, 1 (1972); G. E. Busch and K. R. Wilson, J. Chem. Phys. **56**, 3638 (1972); R. N. Zare and D. R. Hershback, Proc. IEEE **51**, 173 (1963).

[25] In all the systems we have studied, only parallel transitions have been observed. That is the case for the $Kr \cdot H_2O^+$ as well.

[26] M. F. Jarrold, A. J. Illies, and M. T. Bowers, J. Chem. Phys. **79**, 6086 (1983).

[27] M. F. Jarrold, A. J. Illies, and M. T. Bowers, J. Chem. Phys. **82**, 1832 (1985).

[28] W. J. Chesnavich and M. T. Bowers, J. Am. Chem. Soc. **98**, 8301 (1976); Prog. React. Kinetics **11**, 137 (1982).

[29] A. J. Illies, M. F. Jarrold, W. Wagner-Redeker, and M. T. Bowers, J. Phys. Chem. **88**, 5204 (1984).

[30] H-S. Kim, M. F. Jarrold, and M. T. Bowers, J. Chem. Phys. **90**, 3584 (1986).

[31] J. Snodgrass and M. T. Bowers (to be published).